

# Evidence for two-gap nodeless superconductivity in $\text{SmFeAsO}_{0.8}\text{F}_{0.2}$ from point-contact Andreev-reflection spectroscopy

D Daghero,<sup>1</sup> M Tortello,<sup>1</sup> R S. Gonnelli,<sup>1</sup> V A Stepanov,<sup>2</sup> N D Zhigadlo,<sup>3</sup> and J Karpinski<sup>3</sup>

<sup>1</sup>Dipartimento di Fisica and CNISM, Politecnico di Torino, 10129 Torino, Italy

<sup>2</sup>P N. Lebedev Physical Institute, Russian Academy of Sciences, 119991 Moscow, Russia

<sup>3</sup>Laboratory for Solid State Physics, ETHZ, CH-8093 Zurich, Switzerland

Point-contact Andreev-reflection measurements were performed in  $\text{SmFeAsO}_{0.8}\text{F}_{0.2}$  polycrystals with  $T_c = 53$  K. The experimental conductance curves reproducibly exhibit peaks around 6 mV and shoulders at  $V = 16-20$  mV, indicating the presence of two nodeless superconducting gaps. While the single-band Blandier-Tinkham-Klapwijk fit can only reproduce a small central portion of the conductance curve, the two-gap one accounts remarkably well for the shape of the whole experimental  $dI/dV$ . The fit of the normalized curves give  $\Delta_1(0) = 6.15 \pm 0.45$  meV and  $\Delta_2(0) = 18 \pm 3$  meV. Both gaps close at the same temperature and follow a BCS-like behavior.

PACS numbers: 74.50.+r, 74.70.Dd, 74.45.+c

The experimental evidence of superconductivity in F-doped  $\text{LaFeAsO}$  [1] opened the way to the discovery of a new class of superconductors that, with the exception of the copper-based high- $T_c$  superconductors, show the highest superconducting critical temperatures known so far, with a record  $T_c$  of 55 K in F-doped or oxygen deficient  $\text{SmFeAsO}$  [2, 3].

Similarly to  $\text{LaFeAsO}$  [4],  $\text{SmFeAsO}$  is semimetallic and shows a spin-density-wave (SDW) antiferromagnetic order as well as a tetragonal-to-orthorhombic structural transition at 140 K [5]. Above a critical value of F substitution [5], charge doping on FeAs planes suppresses the SDW order and superconductivity occurs. The vicinity of the superconducting state to a magnetic order raises many questions concerning the pairing mechanism that is responsible for superconductivity. Theoretical calculations [6] for the  $\text{LaFeAsOF}$  system showed that the electron-phonon coupling is not sufficient to explain the observed  $T_c$ . An extended s-wave pairing with a sign reversal of the order parameter between different sheets of the Fermi surface was thus proposed [7] for the same compound and shown to be compatible with a coupling mechanism related to spin fluctuations. On the other hand, a growing evidence for multi-gap superconductivity in FeAs-based compounds is being provided by several experimental works [8, 9, 10, 11, 12, 13, 14, 15, 16].

In this situation, where there is no general consensus concerning the pairing mechanism in these new superconductors, the determination of the number, nature and symmetry of the superconducting order parameter(s) assumes particular importance. In this regard, point-contact Andreev-reflection (PCAR) spectroscopy is a powerful technique to determine the gap value(s) and its (their) symmetry. PCAR measurements performed so far in  $\text{SmFeAsO}_{1-x}\text{F}_x$  [16, 17] are somehow in disagreement with each other: Chen et al. [17] observed a single, BCS-like, s-wave gap while Wang et al. [16] reported two nodal order parameters. Here we report results of point-contact Andreev-reflection measurements on high-

quality polycrystalline samples of  $\text{SmFeAsO}_{0.8}\text{F}_{0.2}$  with  $T_c^{\text{on}} = 53$  K reproducibly showing the presence of two nodeless energy gaps,  $\Delta_1(0) = 6.15 \pm 0.45$  meV and  $\Delta_2(0) = 18 \pm 3$  meV; both gaps show a BCS-like temperature dependence and close at the same temperature, always very close to the bulk  $T_c$  measured by susceptibility and resistivity.

The polycrystalline samples of  $\text{SmFeAsO}_{0.8}\text{F}_{0.2}$  were synthesized under high pressure starting from SmAs, FeAs,  $\text{SmF}_3$ ,  $\text{Fe}_2\text{O}_3$  and Fe. After the materials were pulverized and sealed in a BN crucible, a pressure of 30 kbar was applied at room temperature. The temperature was then increased within 1 h up to 1350–1450 °C, kept for 4.5 h and quenched back to room temperature. Finally the pressure was released. The resulting samples are very compact and made up of shiny crystallites whose size, as revealed by SEM images, is of the order of 30 μm. The onset of the magnetic (resistive) transition is 52.1 K (53.0 K), as shown in the insets of Fig. 1.

Instead of a metallic tip pressed against the sample as in the standard PCAR technique, we made the point contacts by placing a small drop of Ag conducting paste on the freshly cleaved surface of the sample. This is a pressure-less technique we successfully used in various classes of superconductors, i.e.  $\text{MgB}_2$ ,  $\text{CaC}_6$ , ruthenocuprates, A15 (for details see, for instance, refs. [18] and [19]). It gives much more stable contacts under thermal cycling, which allowed us to easily record the conductance curves up to 200 K.

When performing PCAR experiments, the size of the contact should be smaller than the electronic mean free path,  $\ell$ , in the superconductor [20]. Only in this way the condition for ballistic conduction in the contact is fulfilled and spectroscopy is possible. Although at present the value of  $\ell$  is still not known in this low-carrier-density compound, the presence of clear Andreev-reflection features, the general shape of the conductance curves, the absence of dips [21] and the coincidence between the critical temperature of

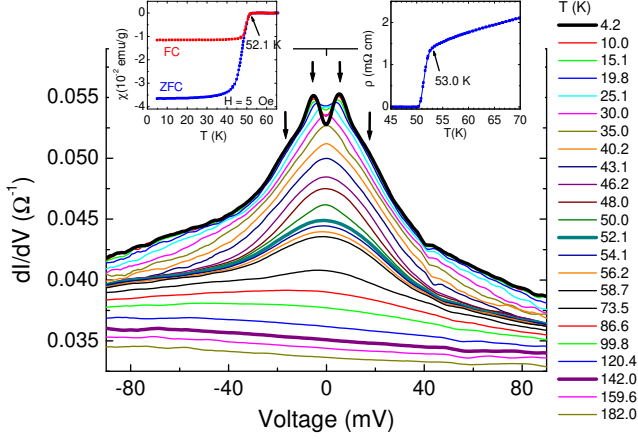


FIG. 1: (color online) Temperature dependence of the raw conductance curves of a point contact with  $T_c = 52$  K. The low-temperature curve (upper thick line) features two peaks and two shoulders (indicated by arrows) related to  $\epsilon_1$  and  $\epsilon_2$ , respectively. The curve at  $T_c$  (middle thick line) has a hump-like shape which attenuates at 140 K (lower thick line). Insets show the resistivity and dc susceptibility of the sample.

the junction and the bulk  $T_c$  indicate that the spectroscopic requirements are satisfied in our measurements.

The differential conductance curves of our point contacts were obtained by taking the numerical derivative of the I-V characteristics. In order to compare the results with a theoretical model, the measured conductance curves of each junction had first to be normalized, i.e. divided by the relevant normal-state conductance. A fit was then performed by means of a two-band modified [22] Blandin-Tinkham-Klapwijk model [23] generalized to take into account the angular distribution of the current injection at the N/S interface [24]. According to this model the normalized conductance is the weighed sum of the conductances of the two bands,  $G = w_1 G_1^{BTK} + (1 - w_1) G_2^{BTK}$  where  $w_1$  is the weight of band 1. Each conductance depends on 3 parameters: the gap value,  $\Delta$ , a broadening parameter,  $\Gamma$  [22], and the barrier parameter  $Z$  that accounts for both the height of the potential barrier and the mismatch of the Fermi velocities at the N/S interface [23, 24]. Although the model contains 7 fitting parameters (3 for each band plus  $w_1$ ), they are not totally free in the sense that, if one fits the whole temperature dependence of a conductance curve, the two barrier parameters  $Z_1$  and  $Z_2$  as well as the weight  $w_1$  should be kept constant with increasing temperature, while the broadening parameters  $\Gamma_1$  and  $\Gamma_2$  should remain almost constant, or increase at  $T > T_c = 2$ . These requests automatically restrict the variability of these parameters.

Figure 1 shows the raw conductance curves of a 28-ohm contact, measured from 4.2 K up to about 180 K. The critical temperature of the junction is 52 K. The

low-temperature curve (upper thick line) shows clear Andreev-reflection features such as two peaks at  $\pm 6$  mV, certainly related to a superconducting gap [17], plus two pronounced shoulders at higher bias voltages that, in a way very similar to what previously observed in  $\text{MgB}_2$  [18], can indicate the presence of a second, larger gap (this indication will be further substantiated in the following, by fitting the conductance curves up to  $T_c$  and observing the temperature evolution of the gaps). In all our contacts, the normal-state conductance curve measured at  $T_c$  (middle thick line in Fig. 1) features a hump at zero bias that gradually decreases with increasing temperature until it completely disappears (lower thick line) around the Neel temperature of the parent compound,  $T_N = 140$  K [5]. This might suggest a magnetic origin of this hump. A similar downward curvature of the normal-state spectrum was also found in recent PCAR [10] and ARPES [9] measurements in  $\text{Ba}_{0.6}\text{K}_{0.4}\text{Fe}_2\text{As}_2$ . Finally, the conductance is asymmetric (higher at negative bias, i.e. when electrons are injected into the superconductor) at all temperatures, even above  $T_c$ . This asymmetry, clearly visible in Fig. 1, was also observed in other PCAR measurements [10, 11] and is most probably related to the fast decrease of the density of states at the Fermi level [26]. Note that the asymmetry persists even when the zero-bias hump disappears.

Figure 2 shows several examples of low-temperature normalized conductance curves (symbols). Since the upper critical field,  $H_{c2}$ , is certainly very high [25], the normal state conductance at  $T < T_c$  is not experimentally accessible. The normalization was therefore performed by using the normal-state conductance curve measured at the critical temperature of the junction. The contact resistance  $R_N$ , indicated in the labels of each panel, decreases from top to bottom. In all cases the one-gap BTK fit (dash lines) is compared to the two-gap one (solid lines). It is clear that the quality of the fit performed with the one-gap model is quite poor and can account only for a small central portion of the curve (as in Ref. [17]). The resulting values of the gap range between 6.45 and 8.9 meV, corresponding to  $2\langle 0 \rangle = k_B T_c = 2.9$ –3.9. The two-gap fit can instead reproduce the measured conductances remarkably well and gives values of 5.7–6.6 meV for the small gap, and of 16–21 meV for the large one. In most cases, the amplitude of the Andreev signal (height of the curves) is of the order of 20–30 % (similar to what observed in Refs. [17, 18, 19]) and gives clear and unambiguous measurements; the ratio  $\langle 0 \rangle = \langle 0 \rangle / \langle 0 \rangle$  was usually 0.5–0.6 or smaller;  $w_1$  was 0.55–0.10 depending on the junction. The normalized conductances often show a residual asymmetry between the left and the right part which mainly affects the determination of the larger gap; this asymmetry might be due to the aforementioned unconventional shape of the background which is itself asymmetric and changes with temperature. When possible, a fit of both sides of the

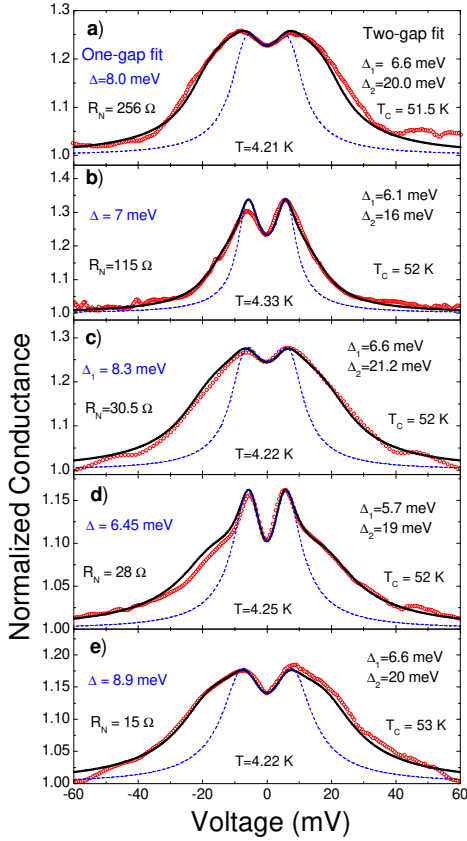


FIG. 2: (color online) (a) to (e): normalized conductance curves (symbols) at 4.2 K in  $\text{SmFeAsO}_{0.8}\text{F}_{0.2}$ . The contact resistance,  $R_N$ , decreases from top to bottom. The curves are reported together with their relevant one-gap (dash lines) and two-gap (solid lines) BTK fits. The gap values are indicated on the left (single-gap fit) and on the right (two-gap fit).

normalized curves was done in order to determine the spread of  $\Delta_2$  values arising from this asymmetry.

Several point-contact measurements on FeAs-based superconductors reported a dependence of the conductance curves on the contact resistance and, therefore, on the pressure applied by the tip with the consequent appearance of additional structures, mainly zero-bias conductance peaks (ZBCP), not related to the superconducting gaps [17, 27]. As clearly shown in Fig. 2, this problem is completely overcome in our point contacts, where no pressure is applied to the sample. The general shape of our curves is rather independent on the contact resistance (as expected for ballistic junctions) and the extracted gap values are in good agreement with each other even for very different contact resistances (see, for example, the curves in panel (a) and (e) of Fig. 2). The systematic absence of zero-bias peaks in our curves completely rules out the d-wave symmetry for the gaps. As a matter of fact it can be easily shown that, in the case of a d-wave gap, all the conductance curves calculated within the generalized BTK model [24] using  $\Delta(0) = \Delta(0) = 0.5 - 0.6$  and  $Z$  values

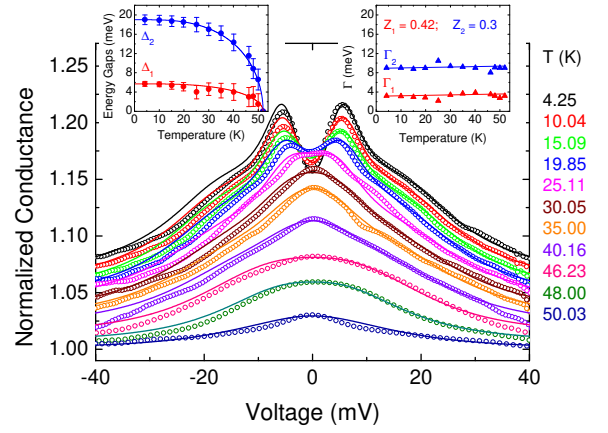


FIG. 3: (color online) Temperature dependence of the normalized conductance curves (symbols) together with their relevant two-gap BTK fits (lines). The curves are vertically shifted for clarity. The raw data are those shown in Fig. 1 and the insets show the temperature dependency of the gaps ( $\Delta_1$  and  $\Delta_2$ ) and of the broadening parameters ( $\Gamma_1$  and  $\Gamma_2$ ) given by the two-gap fit.

similar to the experimental ones ( $Z = 0.3-0.4$ ), show clear ZBCP at 4.2 K whenever the direction of injection of the current forms an angle  $> 15^\circ$  with respect to the anti-nodal direction [28]. If the gaps had d-wave symmetry, the experimental absence of ZBCP would mean that the current was always injected within  $15^\circ$  of the anti-nodal direction, which is absolutely unreasonable in the case of polycrystalline samples.

In order to obtain the behavior of the two gaps as a function of temperature, a fit of the temperature dependence of the normalized conductance curves was performed with the two-band BTK model. A typical result is shown in Fig. 3 where the experimental data (symbols) are compared to the relevant BTK curves (lines) that best fit the positive-bias side. The barrier parameters  $Z_1$  and  $Z_2$  used for the fit are indicated in the label of the right inset; a small decrease (of the order of 20% of these values) had to be allowed to obtain a good fit of the whole temperature dependence, but this might simply mean that the normal-state conductance at low temperature is more peaked than that at  $T_C$ . The values of the gaps  $\Delta_1$  and  $\Delta_2$  and of the broadening parameters  $\Gamma_1$  and  $\Gamma_2$  are reported in the insets. Note that the temperature dependence of the gaps is impressively BCS-like, with gap ratios  $2\Delta_1(0)/k_B T_C = 2.55$  and  $2\Delta_2(0)/k_B T_C = 8.5$ . Here, error bars indicate the uncertainty on the gaps due to the fit and the experimental resolution of the technique,  $k_B T$ .

The temperature dependence of the gaps obtained from the two-gap BTK fit of the curves shown in Figure 3 and from various other measurements is reported in Figure 4. The reproducibility of the small gap (open symbols) is noticeable:  $\Delta_1$  is close to 6 meV at low temperature and follows a BCS-like trend up to the critical temperature which was always between 50 and 53 K (the

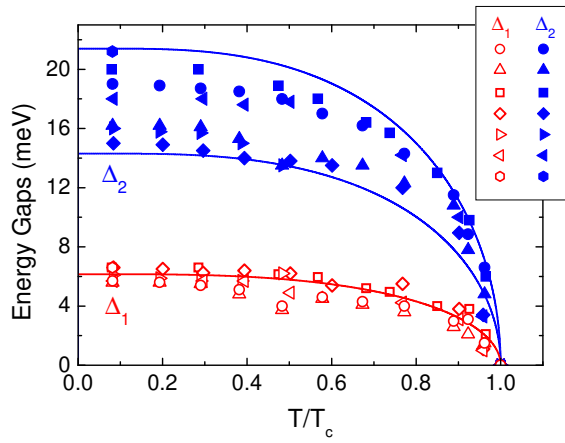


FIG. 4: (color online) Temperature dependence of the gaps  $\Delta_1$  (open symbols) and  $\Delta_2$  (filled symbols) as extracted from the two-gap fit of the conductance curves. Lines are BCS-like curves. Details are in the text.

normalized temperature  $T/T_c$  is used in Fig.4 for homogeneity). As far as  $\Delta_2$  is concerned, its behaviour in each set of data is nicely BCS, but the spread of values between different data sets is rather wide: all the data fall in a region bounded by two BCS-like curves with gap ratios  $\Delta_2(0)/k_B T_c = 7$  and 9, respectively. Incidentally, this region is centered on a value  $\Delta_2 = 18$  meV that is close to that determined with infrared ellipsometry [29],  $18.5$  meV. The spread of  $\Delta_2$  values shown in Fig.4 cannot be ascribed to our PCAR technique, since in MgB<sub>2</sub>, for example, both the gaps were determined in exactly the same way with a great accuracy ( $0.5$  meV at most, at  $4.2$  K). It is instead a property of this particular compound; it mainly comes from the residual asymmetry of the normalized curves (when the negative/positive bias side of the same curve is fitted). Even though, as explained above, this asymmetry is likely to be due to the shape of the normal state (which possibly becomes more and more asymmetric on decreasing temperature), we cannot exclude other possibilities, i.e. that it is an intrinsic feature of the superconducting state in this material. Finally, notice that at low temperature the ratio of the gaps,  $\Delta_2/\Delta_1$  is  $\sim 3$ . Similar values have also been reported for other pnictide superconductors [10, 11, 12] and might indicate that the proposed interband-only, extended s-wave model [7] cannot fully explain the experimental data since a higher intraband coupling of non-magnetic origin should also be taken into account [30].

In summary, we performed pressure-less PCAR measurements in  $\text{SmFeAsO}_{0.8}\text{F}_{0.2}$  with  $T_c$  up to  $53$  K. The experimental point-contact conductances show peaks around  $6$  mV and clear shoulders at higher bias voltages,  $16 - 20$  mV, indicating the presence of two superconducting gaps. The BTK fit of the low-temperature normalized conductances fully supports this observation:

the single-band fit gives gap values in good agreement with those reported in literature [17] but can only reproduce a small central portion of the conductance curve. The two-gap fit, instead, accounts remarkably well for the shape of the whole experimental curve. Furthermore, the fit of the temperature dependence of the normalized conductance curves gives a BCS-like dependence for both the gaps, which close at the same critical temperature, directly revealing that multi-gap nodeless superconductivity is a fundamental property of this oxypnictide superconductor. Averaging over various contacts, we obtained  $\Delta_1(0) = 6.15 \pm 0.45$  meV and  $\Delta_2(0) = 18.3$  meV with ratios  $\Delta_2(0)/k_B T_c = 2.5 \pm 3$  and  $\Delta_2(0)/k_B T_c = 7.9$ , respectively. This result, together with other experimental findings in pnictide superconductors [8, 9, 10, 11, 12, 13, 14, 15, 16], points therefore towards a common multi-gap scenario to most (if not all) Fe-As-based superconductors.

We thank G.A. Ummarino, I.I. Mazin, P. Szabo, L.F. Cohen and Y. Fasano for useful discussions. V.A.S. acknowledges support by the Russian Foundation for Basic Research Project No. 09-02-00205. This work was done within the PRIN project No. 2006021741.

- 
- [1] Y. Kamihara, et al, J. Am. Chem. Soc. 130, 3296-3297 (2008).
  - [2] Z.A. Ren, et al, Chin. Phys. Lett. 25, 2215 (2008).
  - [3] Z.A. Ren, et al, Europhys. Lett. 83, 17002 (2008).
  - [4] Clarina de la Cruz, et al, Nature, 453, 899 (2008).
  - [5] A.J. Drew et al, arXiv:0807.4876v1.
  - [6] L. Boeri et al, Phys. Rev. Lett. 101, 026403 (2008).
  - [7] I.I. Mazin et al, Phys. Rev. Lett. 101, 057003 (2008).
  - [8] F. Hunte, et al, Nature 453, 903 (2008).
  - [9] H. Ding et al, Europhys. Lett., 83, 47001 (2008).
  - [10] P. Szabo, et al, arXiv:0809.1566v2.
  - [11] R.S. Gonnelli et al, arXiv:0807.3149.
  - [12] S. Kawasaki et al, arXiv:0810.1818v1.
  - [13] K. Matano, et al, Europhys. Lett. 83, 57001 (2008).
  - [14] P. Samuely, et al, arXiv:0806.1672v4.
  - [15] M.H. Pan, et al, arXiv:0808.0895.
  - [16] Y. Wang, et al, Supercond. Sci. Technol. 015018 (2009).
  - [17] T.Y. Chen, et al, Nature, 453, 1224 (2008).
  - [18] R.S. Gonnelli et al, Phys. Rev. Lett. 89, 247004 (2002).
  - [19] R.S. Gonnelli et al, Phys. Rev. Lett. 100, 207004 (2008).
  - [20] A.M. Duif et al, J. Phys.: Condens. Matter 1, 3157 (1989).
  - [21] G. Sheet et al, Phys. Rev. B. 69, 134507 (2004).
  - [22] A.P. Leenik, et al Phys. Rev. B 49, 10016-10019 (1994).
  - [23] G.E. Blonder, M.Tinkham, T.M. Klapwijk, Phys. Rev. B 25, 4515 (1982).
  - [24] S. Kashiwaya, et al, Phys. Rev. B 53, 2667-2676 (1996).
  - [25] C. Senatore et al, Phys. Rev. B. 78, 054514 (2008).
  - [26] D.J. Singh and M.-H. Du, Phys. Rev. Lett. 100, 237003 (2008).
  - [27] K.A. Yates, et al, Supercond. Sci. Technol. 21, 092003 (2008).
  - [28] N. Stefanakis, J. Phys.: Condens. Matter, 13, 1265

- (2001).
- [29] A. Dubroka et al, Phys Rev. Lett., 101, 097011 (2008).
- [30] O. V. Dolgov et al, arXiv:0810.1476v1